Biomedical Optics EXPRESS

# Multimodal microscopy with sub-30 fs Yb fiber laser oscillator

**Bai Nie,[1,4] Ilyas Saytashev,[1,4] Andy Chong,[2] Hui Liu,[2] Sergey N. Arkhipov,[1] Frank W. Wise,[2] and Marcos Dantus[1,3,*]**

[1]*Department of Chemistry, Michigan State University, East Lansing, Michigan 48824, USA*
[2]*Department of applied physics, Cornell University, Ithaca, New York 14853, USA*
[3]*Biophotonic Solutions Inc., 1401 E. Lansing Drive, Suite 112, East Lansing, Michigan 48823, USA*
[4]*Contributed equally to this work.*
**dantus@chemistry.msu.edu*

**Abstract:** Nonlinear optical microscopy with sub-30 fs pulses from an Yb-fiber laser, approximately three times shorter than typical fiber laser pulses, leads to an order of magnitude brighter third harmonic generation imaging. Multiphoton fluorescence, second and third harmonic generation modalities are compared on stained microspheres and unstained biological tissues.



**OCIS codes:** (180.4315) Nonlinear microscopy; (060.2320) Fiber optics amplifiers and oscillators; (110.2350) Fiber optics imaging.

## References and links

1. W. Denk, J. H. Strickler, and W. W. Webb, "Two-photon laser scanning fluorescence microscopy," Science **248**(4951), 73–76 (1990).
2. W. R. Zipfel, R. M. Williams, and W. W. Webb, "Nonlinear magic: multiphoton microscopy in the biosciences," Nat. Biotechnol. **21**(11), 1369–1377 (2003).
3. K. König, "Multiphoton microscopy in life sciences," J. Microsc. **200**(2), 83–104 (2000).
4. S. Maiti, J. B. Shear, R. M. Williams, W. R. Zipfel, and W. W. Webb, "Measuring serotonin distribution in live cells with three-photon excitation," Science **275**(5299), 530–532 (1997).
5. Y. Barad, H. Eisenberg, M. Horowitz, and Y. Silberberg, "Nonlinear scanning laser microscopy by third harmonic generation," Appl. Phys. Lett. **70**(8), 922–924 (1997).
6. J. A. Squier, M. Muller, G. J. Brakenhoff, and K. R. Wilson, "Third harmonic generation microscopy," Opt. Express **3**(9), 315–324 (1998).
7. P. Xi, Y. Andegeko, D. Pestov, V. V. Lovozoy, and M. Dantus, "Two-photon imaging using adaptive phase compensated ultrashort laser pulses," J. Biomed. Opt. **14**(1), 014002 (2009).
8. D. Yelin, D. Oron, E. Korkotian, M. Segal, and Y. Silberberg, "Third-harmonic microscopy with a titanium-sapphire laser," Appl. Phys. B **74**(9), S97–S101 (2002).
9. C. K. Sun, S. W. Chu, S. P. Tai, S. Keller, U. K. Mishra, and S. P. DenBaars, "Scanning second-harmonic/third-harmonic generation microscopy of gallium nitride," Appl. Phys. Lett. **77**(15), 2331–2333 (2000).
10. A. Chong, J. Buckley, W. Renninger, and F. Wise, "All-normal-dispersion femtosecond fiber laser," Opt. Express **14**(21), 10095–10100 (2006).
11. W. H. Renninger, A. Chong, and F. W. Wise, "Self-similar pulse evolution in an all-normal-dispersion laser," Phys. Rev. A **82**(2), 021805 (2010).
12. B. Nie, D. Pestov, F. W. Wise, and M. Dantus, "Generation of 42-fs and 10-nJ pulses from a fiber laser with self-similar evolution in the gain segment," Opt. Express **19**(13), 12074–12080 (2011).
13. A. C. Millard, P. W. Wiseman, D. N. Fittinghoff, K. R. Wilson, J. A. Squier, and M. Müller, "Third-harmonic generation microscopy by use of a compact, femtosecond fiber laser source," Appl. Opt. **38**(36), 7393–7397 (1999).
14. G. J. Liu, K. Kieu, F. W. Wise, and Z. P. Chen, "Multiphoton microscopy system with a compact fiber-based femtosecond-pulse laser and handheld probe," J Biophotonics **4**(1-2), 34–39 (2011).
15. A. Besaratinia, J. I. Yoon, C. Schroeder, S. E. Bradforth, M. Cockburn, and G. P. Pfeifer, "Wavelength dependence of ultraviolet radiation-induced DNA damage as determined by laser irradiation suggests that cyclobutane pyrimidine dimers are the principal DNA lesions produced by terrestrial sunlight," FASEB J. **25**(9), 3079–3091 (2011).
16. D. Kobat, M. E. Durst, N. Nishimura, A. W. Wong, C. B. Schaffer, and C. Xu, "Deep tissue multiphoton microscopy using longer wavelength excitation," Opt. Express **17**(16), 13354–13364 (2009).
17. A. Chong, H. Liu, B. Nie, B. G. Bale, S. Wabnitz, W. H. Renninger, M. Dantus, and F. W. Wise, "Pulse generation without gain-bandwidth limitation in a laser with self-similar evolution," Opt. Express **20**(13), 14213 –14220 (2012).

#167236 - $15.00 USD Received 25 Apr 2012; revised 8 Jun 2012; accepted 9 Jun 2012; published 27 Jun 2012

18. V. V. Lozovoy, I. Pastirk, and M. Dantus, "Multiphoton intrapulse interference. IV. Ultrashort laser pulse spectral phase characterization and compensation," Opt. Lett. **29**(7), 775–777 (2004).
19. B. Xu, J. M. Gunn, J. M. D. Cruz, V. V. Lozovoy, and M. Dantus, "Quantitative investigation of the multiphoton intrapulse interference phase scan method for simultaneous phase measurement and compensation of femtosecond laser pulses," J. Opt. Soc. Am. B **23**(4), 750–759 (2006).
20. D. Pestov, V. V. Lozovoy, and M. Dantus, "Multiple Independent Comb Shaping (MICS): phase-only generation of optical pulse sequences," Opt. Express **17**(16), 14351–14361 (2009).
21. M. M. Wefers and K. A. Nelson, "Space-time profiles of shaped ultrafast optical waveforms," IEEE J. Quantum Electron. **32**(1), 161–172 (1996).
22. F. Frei, A. Galler, and T. Feurer, "Space-time coupling in femtosecond pulse shaping and its effects on coherent control," J. Chem. Phys. **130**(3), 034302 (2009).
23. D. Brinks, F. D. Stefani, and N. F. Hulst, "Nanoscale spatial effects of pulse shaping," Ultrafast Phenomena XVI **92**, 890–892 (2009).
24. N. Krebs, R. A. Probst, and E. Riedle, "Sub-20 fs pulses shaped directly in the UV by an acousto-optic programmable dispersive filter," Opt. Express **18**(6), 6164–6171 (2010).

## 1. Introduction

Due to benefits such as high contrast ratio, submicron resolution and depth resolved imaging, multiphoton microscopy has gained broad acceptance in recent years [1–3]. Modalities such as two-photon excited fluorescence (TPEF) [4], second harmonic generation (SHG) and third harmonic generation (THG) microscopy [5,6] provide complementary information for stained as well as unstained samples. SHG and THG microscopy depend on molecular properties and require no fluorescent labeling, thereby reducing the complexity of biological imaging. Signal is known to increase as the inverse of pulse duration for SHG [2] and the inverse of the pulse duration squared for THG, without bandwidth limits imposed by the two-photon absorption spectrum; making SHG and THG amenable to ultrashort pulse excitation. Laser pulse duration dependence has been confirmed for two-photon microscopy down to 10 fs pulses [7].

Different ultrafast solid state laser sources, such as Ti:sapphire at 800 nm [8], Cr:forsterite at 1230 nm [9] and OPO at 1500 nm [5], have been used for third harmonic generation microscopy. In the past decade, compact fiber lasers have drawn increasing attention due to their compact size and greater stability [10–12]. Er fiber at 1550 nm [13] and Yb fiber at 1060 nm [14] have been used for multiphoton microscopy; however, these lasers have pulse durations greater than 100 fs. While sub-10 fs pulses are readily available from Ti:sapphire sources, the THG signal from such sources is near 270 nm, a wavelength that is absorbed by biological tissue, especially DNA [15]. In order to avoid laser induced damage to living tissue and enable microscopic imaging deeper into living tissue, interest has shifted towards imaging using longer wavelength sources [16].

Here we test a new fiber laser source delivering a very broadband spectrum centered at 1030 nm. The output pulses can be de-chirped to as short as ~21 fs [17] using a pulse shaper with Multiphoton Intrapulse Interference Phase Scan (MIIPS) [18–20]. To the best of our knowledge, this is the shortest pulse duration obtained directly from a fiber oscillator. This source is evaluated for multi-modal microscopy using fluorescent polystyrene microspheres and unstained biological samples including guppy fish (Poecilia reticulata) tails and fruit fly (Drosophila melanogaster) wings. Images generated by multiphoton fluorescence, SHG and THG are compared.

## 2. Experimental setup

The experimental setup shown in Fig. 1 consists of an Yb fiber laser oscillator (Fig. 1(a)) that generates a broadband spectrum centered at 1030 nm with ~50 mW average output power at a repetition rate of 62 MHz. It is based on an all-normal dispersion cavity scheme [11] where self-similar amplification takes place in the gain medium. The pulses gain energy and bandwidth while evolving into a parabolic temporal profile in the gain segment [11] and maintain the parabolic profile in the PCF segment with the temporal and spectrum bandwidth increasing. The condition for self-similar amplification is facilitated by introducing a narrow spectral filter consisting of a grating and a collimator [11]. The self-similar pulses are further

#167236 - $15.00 USD Received 25 Apr 2012; revised 8 Jun 2012; accepted 9 Jun 2012; published 27 Jun 2012

extended in both temporal and spectral domains by an intra-cavity segment of normal dispersion photonic crystal fiber (PCF). This novel scheme enables the laser spectral bandwidth to exceed the gain bandwidth and leads to pulse durations as short as 20 fs. The detailed design and principle of the fiber laser is discussed in Ref [17].

A folded 4f pulse shaper (MIIPS Box 640, Biophotonic Solutions) (Fig. 1(b)), with a dual mask 640-pixel spatial light modulator, is used to measure and compensate the dispersion of the output pulses at the focal plane of the microscope (Fig. 1(c)) [18,19]. The results obtained using MIIPS for automated pulse compression are confirmed by interferometric autocorrelation and by theoretical calculation. Due to the diffraction efficiency of the grating and reflection losses by the mirrors inside the shaper, the average power out of the shaper is ~25 mW.

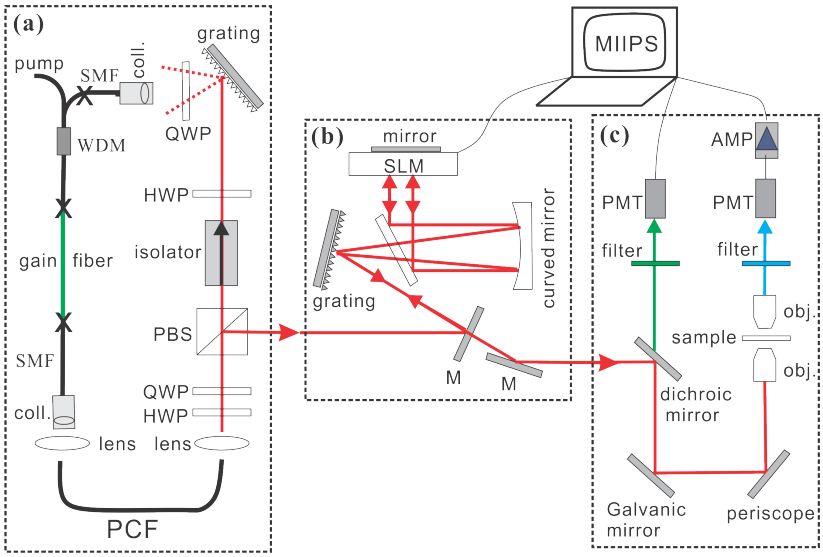


Fig. 1. Schematic of imaging setup. (a) Fiber laser cavity layout. PCF: photonic crystal fiber; SMF: single mode fiber; WDM: wavelength-division multiplexer; HWP and QWP: half- and quarter-waveplate; PBS: polarization beam splitter. (b) 4f-folded pulse shaper. SLM: spatial light modulator; M: mirror. (c) Microscopy setup. AMP: amplifier; PMT: photomultiplier tube.

The laser beam is raster scanned by a pair of mirrors mounted on galvanometers (QuantumDrive-1500, Nutfiled Technology, Inc.) and coupled into a water-immersed objective (Zeiss LD C-APOCHROMAT 40x/1.1) mounted on an adapted Nikon TE-200 inverted microscope. Laser pulses are compressed to their transform limit at the focus of the objective. With the sample placed at the focus of the objective, the SHG generated or TPEF emissions are collected in the Epi direction. SHG/TPEF signal is separated from the fundamental light using a dichroic mirror (700DCSPXR, Chroma Technology Corp.) and is further filtered by a short-pass emission filter (ET680-SP-2P8, Chroma Technology Corp.). A photomultiplier (PMT, HC20-05MOD, Hamamatsu) is used to collect the SHG/TPEF signal. THG, which is primarily generated in the forward direction, is collected by a UV compatible objective (HP ReflX, NT59-886, NA 0.28, focal length 13.3 mm, transmission more than 85% from 200 nm to 700 nm, Edmund Optics). The THG signal is also separated from the excitation light by a UV-pass filter (UG11, transmission from 250 nm to 400 nm) and detected by a PMT (H10720-210, Hamamatsu) whose signal is amplified (SRS445, Stanford Research Systems). Tens of frames are taken to generate one image and each of the frames takes one second to acquire.

The spectrum of the laser pulses, after transmission through the microscope objective, is shown in Fig. 2(a). Dispersion compensation for the laser as well as the microscope objective

#167236 - $15.00 USD Received 25 Apr 2012; revised 8 Jun 2012; accepted 9 Jun 2012; published 27 Jun 2012

is achieved using MIIPS software [18,19]. Briefly, the pulse shaper scans reference phase functions across the spectrum of the pulses and uses the SHG spectral information (generated by a KDP crystal mounted at the focal plane of the objective) to measure the second derivative of the spectral phase. Through double integration of the measurement the system determines the dispersion that needs to be corrected and the pulse shaper implements the correction. Typically, each measurement and compression iteration corrects ~80% of the total dispersion. After a few iterations the pulses are compressed to the theoretical transform limit, as defined by the Fourier transformation of the fundamental laser spectrum. In order to confirm that the compression is complete, the measured SHG spectrum is compared with calculated results based on the fundamental laser spectrum and assuming no phase distortions. The excellent agreement between the calculated and experimentally measured SHG spectra in both linear and log-10 scale is shown in Fig. 2(b) and 2(c).

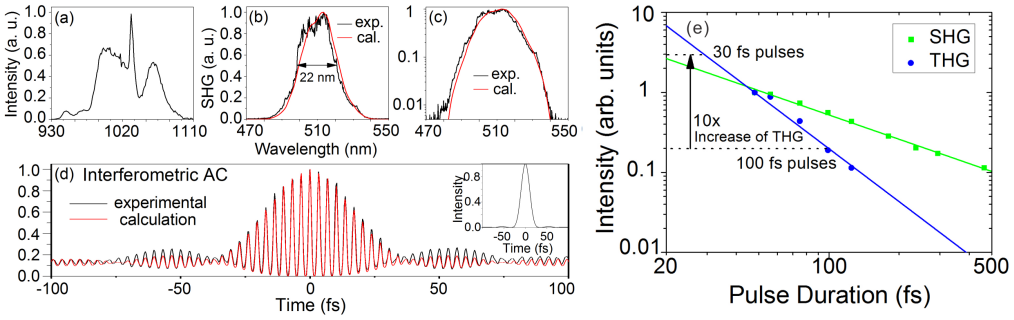


Fig. 2. (a) Laser spectrum after the microscope objective. (b) Comparison of experimental (black) and calculated (red) SHG spectrum on linear scale. (c) Comparison of SHG spectrum on Log-10 scale. (d) Comparison of experimental (black) and calculated (red) interferometric autocorrelation trace. Insert: calculated temporal profile based on the measured laser spectrum (e) Dependence of intensity of SHG (green) and THG (blue) on laser pulse duration. Spots: experimental results; Lines: fitting of experimental data.

After pulse compression, the pulse shaper is used to create two pulse replicas and scan one of them in time to obtain an in situ interferometric autocorrelation at the focal plane of the objective [20]. The full-width at half-maximum (FWHM) duration of the experimental interferometric autocorrelation, shown in Fig. 2(d), is 38 fs corresponding to FWHM pulse duration of 27 fs. This pulse duration is confirmed by comparing experimental (black) and calculated (red) interferometric autocorrelation traces, as shown in Fig. 2(d). The small wings on the transform limited pulse are caused by the sharp features of the laser spectrum (Fig. 1(a)). According to the calculated temporal profile based on the measured laser spectrum, there is around 95% pulse energy within the main pulse. The measured pulse duration after the microscope objective is longer than the 21 fs measured for the compressed pulse duration measured before the objective. The additional pulse broadening is caused by the reduced transmittance of the objective [17] (70% to 50% in the 950 nm to 1150 nm spectral range). After compression and characterization, the KDP crystal is replaced with the microscopy samples. Bright-field imaging is used to ascertain location of samples at the objective focus.

The dependence of SHG and THG intensity on laser pulse duration is also experimentally measured to confirm theoretical expectation. For these measurements the laser beam is focused using a 20x objective on either a BBO crystal to generate SHG signal or on a 1 mm thick glass slide to generate THG. Signals are collected using a spectrometer and integrated. Pulse duration is controlled by adding second order dispersion (linear chirp) to the laser pulses using the pulse shaper. Both SHG and THG signals, normalized at 50 fs, decrease with increasing pulse duration as shown in Fig. 2(e). SHG intensity changes according to $\tau^{-1.01}$ (slope = –1.01 ± 0.02), while THG intensity changes according to $\tau^{-2.2}$ (slope = –2.20 ± 0.2).

#167236 - $15.00 USD Received 25 Apr 2012; revised 8 Jun 2012; accepted 9 Jun 2012; published 27 Jun 2012

These values agree with the theoretical expectation. The slight deviation found for THG is probably caused by the lower signal to noise ratio of the measurements.

## 3. Results

Fluorescein (emission from 470 nm to 650 nm) stained polystyrene microspheres (Fluoresbrite® YG Carboxylate Microspheres 6.00μm, Polysciences Inc.) are used to test the system before imaging live tissues. The signal in the Epi detection corresponds to TPEF, and the signal in the forward direction corresponds to THG. The galvanic mirrors control the area of the sample imaged, as shown in Fig. 3. Comparing the images generated by TPEF and THG in Fig. 3(a) and 3(b), we find that THG images have much better contrast. By limiting the scan range (Fig. 3(c)), a ~1 μm feature that arises from the fabrication of the microspheres can be seen on the 6 μm microspheres. The conditions for THG emission in microscopy have been discussed by Silberberg [5], essentially a change in index of refraction is required to break the backward-forward symmetry near the focal plane. The index of refraction of polystyrene is ~1.57 for 1 μm wavelength light, a large change compared to the index of refraction of air ~1. Therefore THG signal is expected and observed from the surface of polystyrene microspheres. Unlike THG, the TPEF signal is due to the emission from fluorescein that coats the microspheres.

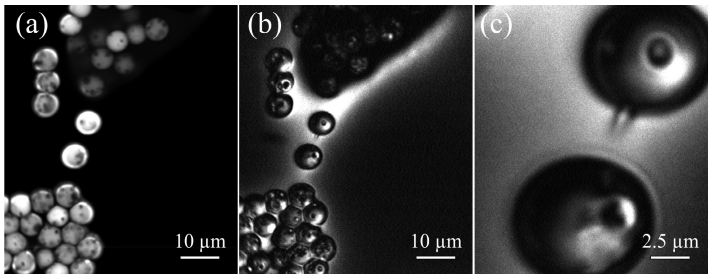


Fig. 3. Multiphoton microscopy images of polystyrene microspheres. (a) Two-photon excited fluorescence (TPEF) image (b) THG image (c) THG image of single bead.

Imaging of biological tissues, unstained samples of fly wings and fish tails, are used to demonstrate the practical relevance of the laser. The samples are mounted on glass slides with Tissue-Tek O.C.T. compound (Sakura, CA) and allowed to immobilize for 30min before imaging. The laser intensity used for imaging the fish tail is 17 mW. The laser power for imaging fly wings is reduced to 7 mW, because higher power is found to damage the sample. Bright-field images were checked before and after imaging to make sure there is no damage on the sample after excitation (Fig. 3(d) and 3(h)). The SHG (Fig. 4(a) and 4(e)) and THG (Fig. 4(b) and 4(f)) images are shown in false color. SHG and THG signals are complementary because they arise from different phase conditions. SHG requires non-centrosymmetric structures while THG requires a change in the index of refraction. By merging the SHG and THG images, we can clearly see the complementary results Figs. 4(c) and 4(g). THG signal from fish tail is not as intense as the SHG signal because of sample thickness. However, there is some complementary information at the edge of the cells provided in the THG images, which is due to the enhanced THG at the interface. For fly wing, THG signals are strongest from the fine hairs on the wing while SHG signal is strongest from the chitin surfaces. Note that the use of sub-30fs pulses resulted in comparable SHG and THG signal levels from fruit fly wings even when using only ~0.1 nJ pulse energy from a fiber laser.

Given that a good spatial mode is required for microscopy, there has been some concern whether 4*f* pulse shapers introduce obvious spatial distortion due to space-time coupling (STC). There have been a number of studies about STC caused by 4*f* pulse shapers and by acousto-optic programmable dispersive filters (AOPDF) in the past two decades [21–24].

#167236 - $15.00 USD Received 25 Apr 2012; revised 8 Jun 2012; accepted 9 Jun 2012; published 27 Jun 2012

According to ref [22], under pure phase modulation introduced by a 4*f* pulse shaper, the beam profile at the focal plane of the objective is only determined by the incident beam profile. STC would only affect the temporal profile of the beam at the focal plane, and would result in a spatially dependent frequency shift. This magnitude of the shift, is described by Eq. (1), and is proportional to the beam size of a monochromatic beam on the SLM ( $2w_0^{SLM}$ ) and inversely proportional to the number of SLM pixels ( $N$ ) covered by the input laser spectrum. Here, $\Delta x_p$ is the SLM pixel size, and $\sigma_\omega$ is the full bandwidth of the incident laser.

$$\Delta\Omega \approx (\sigma_\omega / N)(2w_0^{SLM} / \Delta x_p). \quad (1)$$

In our experiment, $N \approx 600$, $2w_0^{SLM} \approx \Delta x_p$. The ratio ( $\Delta\Omega / \sigma_\omega$ ) between the frequency shift and the full laser bandwidth is only ~0.17%. This minor distortion would be hard to measure and can be ignored. From Eq. (1) we also note that, the frequency shift is equal to the spectral resolution of the shaper ( $\sigma_\omega / N$ ) when $2w_0^{SLM} = \Delta x_p$. Further reducing the spot size of a monochromatic beam on the SLM would not help to reduce the frequency shift, which is limited by the shaper resolution. Hence, we confirm STC is negligible for 4f shapers with an optical resolution equal to or smaller than the SLM pixel size.

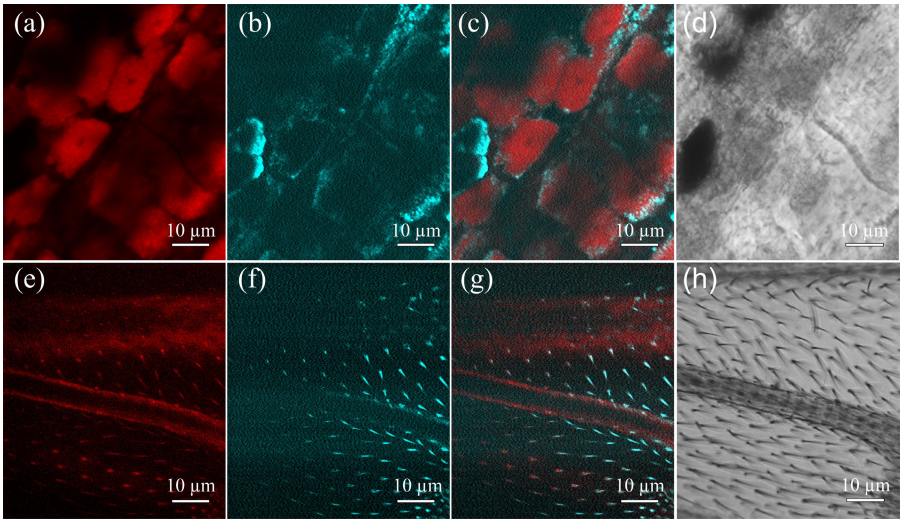


Fig. 4. Multiphoton microscopy images of live tissues. (False color) Top line: images of a guppy fish (Poecilia reticulata) tail. (a) SHG image (green) (b) THG image (blue) (c) Composition of SHG and THG images. (d) Bright-field microscope image. Bottom line: images of fruit fly (Drosophila melanogaster) wings. (e) SHG image (false color, red) (f) THG image (false color, Cyan) (g) Composition of SHG and THG images. (h) Bright-field microscope image.

## 4. Conclusion

We have demonstrated the use of a new generation of ultrafast fiber laser oscillator ideally suited for multi-modal biomedical imaging. The shorter pulse durations achieved by the laser greatly enhance two- and three-photon induced modalities in both stained and unstained living tissues. Complementary results of SHG and THG from living tissue are shown under similar laser conditions.


## Acknowledgments

We gratefully acknowledge a valuable discussion about space time coupling with Vadim V. Lozovoy from the Dantus group. The Dantus Research Group gratefully acknowledges

support from the National Science Foundation CRIF: Instrument Development grant 0923957 for the development of next-generation laser sources for biomedical imaging, and support from the National Institute of Health (Grant No. EB008843), for the evaluation of short pulse lasers for biomedical imaging. The Wise Research Group gratefully acknowledges funding from the National Science Foundation (Grant No. ECS-0901323) and the National Institute of Health (Grant No. EB002019).

#167236 - $15.00 USD Received 25 Apr 2012; revised 8 Jun 2012; accepted 9 Jun 2012; published 27 Jun 2012